

# High-level Intellectual Property Obfuscation via Decoy Constants

Levent Aksoy<sup>†</sup>, Quang-Linh Nguyen<sup>‡</sup>, Felipe Almeida<sup>†</sup>, Jaan Raik<sup>†</sup>, Marie-Lise Flottes<sup>‡</sup>, Sophie Dupuis<sup>‡</sup>  
and Samuel Pagliarini<sup>†</sup>

<sup>†</sup>Department of Computer Systems, Tallinn University of Technology, Tallinn, Estonia

Email: {levent.aksoy, felipe.almeida, jaan.raik, samuel.pagliarini}@taltech.ee

<sup>‡</sup>LIRMM, University of Montpellier, Montpellier, France

Email: {quang-linh.nguyen, marie-lise.flottes, sophie.dupuis}@lirmm.fr

*Abstract*—This paper presents a high-level circuit obfuscation technique to prevent the theft of intellectual property (IP) of integrated circuits. In particular, our technique protects a class of circuits that relies on constant multiplications, such as filters and neural networks, where the constants themselves are the IP to be protected. By making use of decoy constants and a key-based scheme, a reverse engineer adversary at an untrusted foundry is rendered incapable of discerning true constants from decoy constants. The time-multiplexed constant multiplication (TMCM) block of such circuits, which realizes the multiplication of an input variable by a constant at a time, is considered as our case study for obfuscation. Furthermore, two TMCM design architectures are taken into account; an implementation using a multiplier and a multiplierless shift-adds implementation. Optimization methods are also applied to reduce the hardware complexity of these architectures. The well-known satisfiability (SAT) and automatic test pattern generation (ATPG) attacks are used to determine the vulnerability of the obfuscated designs. It is observed that the proposed technique incurs small overheads in area, power, and delay that are comparable to the hardware complexity of prominent logic locking methods. Yet, the advantage of our approach is in the insight that constants – instead of arbitrary circuit nodes – become key-protected.

*Index Terms*—hardware obfuscation, reverse engineering, IP obfuscation, SAT attack, digital FIR filter design.

## I. INTRODUCTION

The involvement of multiple entities in the design and fabrication process of integrated circuits (ICs) potentially leads to security threats, such as reverse engineering, overbuilding, and insertion of malicious hardware Trojans [1]–[3]. Many efficient techniques, such as watermarking [4], IC metering [5], IC camouflaging [6], and logic locking [7], have been proposed to address these issues. Among these techniques, logic locking stands out, offering a protection against a diverse array of adversaries [8]. Logic locking inserts additional logic into a circuit, such as XOR/XNOR gates [9], AND/OR gates [10], or look-up tables [11], driven by a secret key, so that the circuit behaves as specified only when the correct key inputs are applied. The logic locking and activation of a locked circuit in the IC design flow are shown in Fig. 1.

Many widely employed circuits, such as artificial neural networks (ANNs) and finite impulse response (FIR) filters, require the multiplication of constant(s) by input variable(s). In these applications, ANN weights and filter coefficients are constants determined beforehand using sophisticated algorithms [12], [13]. These constants are, therefore, an intellectual

property (IP). Hence, there is a clear interest in protecting the constants since they are valuable, perhaps even more so than the circuit architecture, e.g., the number of layers in an ANN or the multiplier and accumulate block in a filter.

The hardware complexity of ANNs and filters increases as the number of neurons and filter coefficients increases, respectively, restricting their applications on design platforms with a limited number of computing resources, such as FPGAs, and on designs having a strict area requirement [14], [15]. To reduce the design area, taking into account an increase in latency, such IPs are generally implemented under a folded architecture re-using the computing resources [16]. In a folded design, the time-multiplexed constant multiplication (TMCM) operation is a fundamental block that realizes the multiplication of an input variable by a single constant selected from a set of multiple constants at a time [17], [18]. Since a design’s layout is inevitably available to an adversary at an untrusted foundry, constants of the TMCM block are vulnerable to reverse engineering even if a logic locking method is employed. Logic locking, despite its popularity, is not particularly well suited for hiding constants or similar design features.

Given the limitations discussed above, the main contribution of this paper is an **obfuscation technique that protects the sensitive constants from an adversary at an untrusted foundry by hiding them among decoy constants using additional logic with keyed inputs**. The proposed technique implements the obfuscation of the TMCM operation at the register-transfer level (RTL) as shown in Fig. 1. This enables a synthesis tool to optimize the design complexity and also promotes resource sharing, as opposed to traditional logic locking methods which are applied post synthesis at gate level. This paper considers two TMCM design architectures referred to as TMCM-MUL and TMCM-SA. While the former utilizes multiplexors and a multiplier, the latter utilizes shifts, adders, subtractors, adders/subtractors (determined by a select input), and multiplexors under a shift-adds architecture, but no multiplier.

The rest of this paper is organized as follows. Section II gives the background concepts on the TMCM block and folded FIR filter design and presents the related work. The proposed TMCM obfuscation technique is described in Section III. Experimental results are presented in Section IV and finally, Section V concludes the paper.

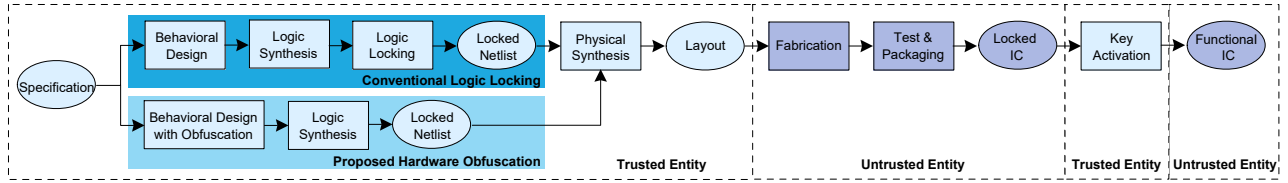


Fig. 1. Conventional logic locking and proposed hardware obfuscation in the IC design flow (adapted from [8]).

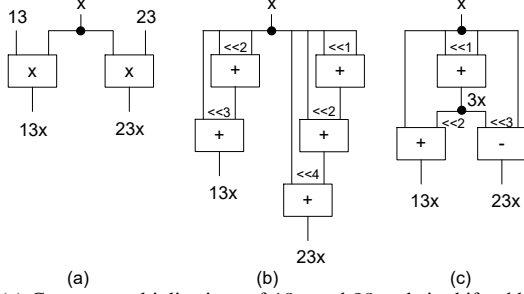


Fig. 2. (a) Constant multiplications of  $13x$  and  $23x$ ; their shift-adds design; (b) DBR method [20]; (c) exact method [22].

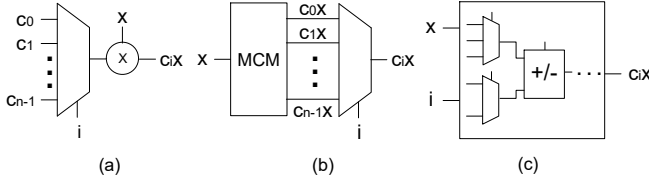


Fig. 3. Design architectures for the implementation of the TMCM operation: (a) *mux-mul*; (b) *mcm-mux*; (c) *mux-add*.

## II. BACKGROUND

### A. Time-Multiplexed Constant Multiplication

Multiplication of constant(s) by input variable(s) is generally realized under a shift-adds architecture using only shifts, adders, and subtractors [19]. Shifts by a constant value can be realized using only wires which represent no hardware cost. A straightforward way of realizing constant multiplications under a shift-adds architecture is the digit-based recoding (DBR) technique [20], which has two main steps: (i) define the constants under a particular number representation, e.g., binary; (ii) for the nonzero digits in the representation of constants, shift the input variables according to digit positions and add/subtract the shifted variables with respect to digit values. As a simple example, consider the multiplication of constants 13 and 23 by the input variable  $x$  in the multiple constant multiplication (MCM) block shown in Fig. 2(a). The decompositions of constants under binary are given as follows:

$$13x = (01101)_{bin}x = x \ll 3 + x \ll 2 + x$$

$$23x = (10111)_{bin}x = x \ll 4 + x \ll 2 + x \ll 1 + x$$

which lead to a multiplierless design with 5 operations as shown in Fig. 2(b). Over the years, algorithms have been proposed for minimizing the number of adders and subtractors by maximizing the sharing of partial products [21]. For our example, the exact algorithm of [22] finds a solution with 3 operations, sharing the subexpression  $3x$  as shown in Fig. 2(c).

On the other hand, the combinational TMCM operation can be implemented under different architectures as shown in Fig. 3 [18]. Given  $n$  constants, the TMCM operation can

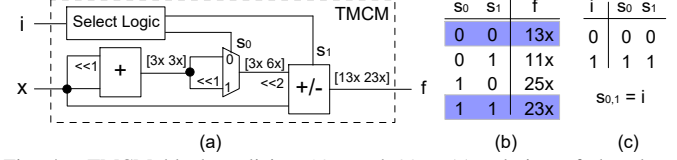


Fig. 4. TMCM block realizing  $13x$  and  $23x$ : (a) solution of the algorithm [18]; (b) outputs based on select inputs of operations; (c) select table.

be implemented using an  $n$ -to-1 multiplexer and a generic multiplier, where the primary select input  $i$  with  $0 \leq i \leq n-1$  determines which constant is multiplied by the input variable (cf. *mux-mul* architecture in Fig. 3(a)). It can also be realized using an MCM block, which implements the multiplications of  $n$  constants by the input variable, and an  $n$ -to-1 multiplexer (cf. *mcm-mux* architecture in Fig. 3(b)). Furthermore, it can be implemented using adders, subtractors, adders/subtractors, and multiplexors (cf. *mux-add* architecture in Fig. 3(c)). Novel methods have been introduced to reduce the hardware complexity of the TMCM operation under the *mux-add* architecture [17], [18]. As a simple example, consider the TMCM operation realizing the constant multiplications of  $13x$  and  $23x$  at a time under the *mux-add* architecture. Fig. 4(a) presents the solution of the algorithm of [18], where the constant multiplications to be computed in time are given between square brackets in order. Note that the adder/subtractor behaves as an adder and a subtractor when its select input is 0 and 1, respectively. All possible values at the output  $f$  of the TMCM operation under the select inputs of the multiplexer and adder/subtractor are given in Fig. 4(b). The TMCM operation can also generate  $11x$  and  $25x$ . To obtain the desired outputs under the primary select input  $i$ , the select logic is required to map  $i$  to the select inputs of the multiplexer and the adder/subtractor, i.e.,  $s_0s_1$ , as shown in Fig. 4(c).

### B. Folded Implementation of Digital FIR Filters

Digital filtering is frequently used in digital signal processing (DSP) applications and FIR filters are generally preferred due to their stability and linear phase property [23]. The output of an  $N$ -tap FIR filter  $y(k)$  is computed as  $\sum_{j=0}^{N-1} h_j \cdot x(k-j)$ , where  $N$  is the filter length,  $h_j$  is the  $j^{\text{th}}$  filter coefficient, and  $x(k-j)$  is the  $j^{\text{th}}$  previous filter input with  $0 \leq j \leq N-1$ . Fig. 5(a) presents the parallel design of the transposed form FIR filter. On the other hand, Fig. 5(b) shows its folded design. The  $\lceil \log_2 N \rceil$ -bit counter counts from 0 to  $N-1$ , generating the timing signal  $TS$  shown in Fig. 5(c). In this figure,  $CLK$  denotes the clock signal fed to all registers which was not shown in Figs. 5(a)-(b) for the sake of clarity. The register block includes  $N-1$  cascaded registers whose counterparts in the parallel design are the ones in the register-add block. Although the complexity of the filter design is reduced under

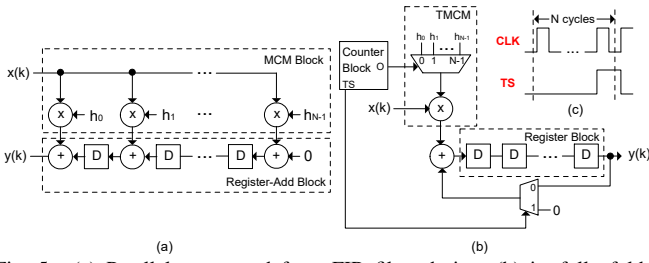


Fig. 5. (a) Parallel transposed form FIR filter design; (b) its fully folded design; (c) the timing signal  $TS$ .

the folded architecture by reusing the common operations, the filter output is obtained in  $N$  clock cycles.

### C. Related Work

Over the years, many defense and attack techniques have been introduced to lock logic circuits and determine the key values of the locked circuits, respectively [24]. Among the attacks against logic locking, the satisfiability (SAT) based attack [25] is a powerful one, which was able to overcome the defenses existing at the time of its publication, such as the logic locking techniques of [9], [10]. In recent years, a large number of SAT attack resilient logic locking methods have been introduced [8], [26].

Efficient hardware obfuscation techniques proposed to protect IPs have been presented in [27]–[29]. For the obfuscation of DSP circuits, a novel approach that uses high-level transformations, a key-based finite-state machine and a reconfigurator was introduced in [30]. The use of decoys in obfuscation has been utilized in [31], but in a manner that is not related to the IP itself, as the decoys are keyed gates. To make the reverse engineering of coefficients of an FIR filter harder for an end-user, adding input and output noises was proposed in [32]. To the best of our knowledge, the use of decoys to hide the target constants of an IP at RTL has not been explored before.

## III. THE PROPOSED OBFUSCATION METHOD

Although target constants can be stored in a tamper-proof memory as the keys in conventional logic locking, this would prevent both sharing of hardware resources and use of a multiplierless design which can lead to a significant reduction in hardware complexity when utilized as shown in Section II-A. Thus, given a set of  $n$  target constants  $\{c_0, c_1, \dots, c_{n-1}\}$ ,  $m$  primary select inputs  $i_0, i_1, \dots, i_{m-1}$ , where  $m = \lceil \log_2 n \rceil$ , and  $p$  key inputs  $k_0, k_1, \dots, k_{p-1}$ , the proposed obfuscation technique initially assigns decoy constants to each target constant in an iterative manner as shown in Algorithm 1. In the *AssignDecoy* function of Algorithm 1, the decoy constants are preferred to have a small Hamming distance with respect to the target constant under the binary representation. This is simply because synthesis tools can also implement constant multiplications under a shift-adds architecture similar to the DBR technique [20] and maximize the sharing of partial products among constant multiplications as shown in Fig. 2. The decoys are selected in between  $[-2^{mbw}, 2^{mbw} - 1]$ , where  $mbw = \lceil \log_2(\max\{|c_j|\}) \rceil$ ,  $0 \leq j \leq n - 1$ , denotes the maximum bit-width of  $n$  target constants. The difference

### Algorithm 1 Assignment of decoys to target constants

**Given:**  $n$  target constants  $\{c_0, c_1, \dots, c_{n-1}\}$  and  $p$  key inputs  
1:  $noi = 0$  ▷ Number of iterations  
2:  $nok = 0$  ▷ Number of used keys  
3: **while**  $nok \neq p$  **do** ▷ Number of decoys to be assigned  
4:  $nod = 2^{noi}$   
5: **for**  $j = 0$  to  $n - 1$  **do**  
6:  $AssignDecoy(c_j, nod)$   
7:  $nok = nok + 1$   
8: **if**  $nok == p$  **then**  
9: **break**  
10:  $noi = noi + 1$

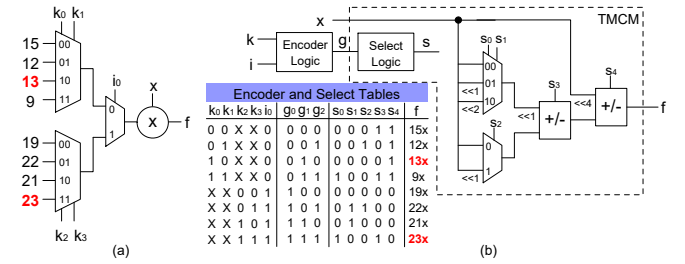


Fig. 6. Obfuscation of the TCMC operation with target constant multiplications of  $13x$  and  $23x$  using decoy constants: (a) TCMC-MUL architecture; (b) TCMC-SA architecture.

on bits between the target and decoy constants starts from the least significant bit. Also, the decoys are decided to be unique to increase the obfuscation. For our example in Fig. 4 with  $n$  is 2, given the number of key inputs  $p$  is 4, for the target constant 13  $(01101)_{bin}$ , the decoys 9  $(01001)_{bin}$ , 12  $(01100)_{bin}$ , and 15  $(01111)_{bin}$  are selected and for the target constant 23  $(10111)_{bin}$ , the decoys 19  $(10011)_{bin}$ , 21  $(10101)_{bin}$ , and 22  $(10110)_{bin}$  are chosen, using a total of 6 decoys.

Then, the obfuscated TCMC operation is implemented based on the given design architecture, i.e., TCMC-MUL or TCMC-SA. The TCMC-MUL architecture is based on the *mux-mul* architecture shown in Fig. 3(a). Initially, for each target constant, a multiplexor is used to select the target and its decoy constant(s) using key input(s). The locations of the target and decoy constants at the multiplexor inputs are determined randomly. The number of inputs of these multiplexors is equal to the number of decoy constants assigned to the target constant plus 1 (denoting the target constant). Then, another multiplexor is used to realize the constant multiplication in the TCMC block in the given order using the primary select input  $i$ . The number of inputs of this multiplexor is equal to  $n$ . Finally, a multiplier is used to realize the constant multiplication. Its size is equal to  $mbw + ibw$ , where  $ibw$  denotes the bit-width of the input variable  $x$ . For our example in Fig. 4, the realization of the obfuscated TCMC block is illustrated in Fig. 6(a). The constant multiplications  $13x$  and  $23x$  are computed when  $k_0 k_1 k_2 k_3 i_0 = 10XX0$  and  $k_0 k_1 k_2 k_3 i_0 = XX111$ , respectively, where  $X$  is the don't care. Note that a wrong key leads to at least one decoy multiplication at a time, e.g., if  $k_0 k_1 k_2 k_3 = 1000$ , the TCMC block generates  $13x$  and  $19x$  when  $i_0$  is 0 and 1, respectively. Hence, in a folded design such as FIR filter in Fig. 5(b), whose TCMC block is obfuscated using the proposed method, a wrong key always generates a wrong output.

The TCMC-SA architecture is based on the *mux-add* architecture shown in Fig. 3(c). Initially, given the order of target and decoy constant multiplications, an encoder logic, which maps the key inputs  $k$  and primary select  $i$  to the select inputs of the TCMC operation, i.e.,  $g$ , is generated. Note that the encoder logic has  $m + p$  inputs and  $\lceil \log_2(n + r) \rceil$  outputs, where  $r$  denotes the total number of decoy constants. Then, the constant multiplications in the same order are given to the algorithm of [18] and an optimized implementation is found under the shift-adds architecture. For our simple example, given the order of target and decoy constant multiplications as in Fig. 6(a), i.e.,  $[15x\ 12x\ 13x\ 9x\ 19x\ 22x\ 21x\ 23x]$ , the realization of the obfuscated TCMC operation is shown in Fig. 6(b) including the encoder and select tables. Note that the select logic, which is implemented by the algorithm of [18] to realize the constant multiplications in a given order, maps the select inputs of the TCMC operation, i.e.,  $g$ , to the select inputs of adders/subtractors and multiplexors in the TCMC design, i.e.,  $s_0s_1s_2s_3s_4$ .

The TCMC operation can also be obfuscated based on the *mcm-mux* architecture shown in Fig. 3(b). In our obfuscated implementation, the MCM block realizes the target and decoy constant multiplications. For each target constant with decoys, a multiplexor is used to select the constant multiplication using the key inputs. Finally, the multiplexor with the primary select input  $i$ , which generates the output, is used. However, in this case, it was observed that the key inputs are so vulnerable to the logic locking attacks since they can be observed easily at the output. The key inputs in the TCMC-MUL and TCMC-SA architectures are behind many logic operators, which is preferred from an obfuscation point of view.

To automate the design and verification process, a computer-aided design (CAD) tool was developed for the obfuscation of the TCMC operation. The CAD tool takes the target constants, the number of key inputs, and the design architecture as inputs, and generates the description of the obfuscated TCMC design in Verilog, the testbench for verification, and synthesis and simulation scripts. Note that the designs under both architectures are described in a behavioral fashion. While targets and decoys are expressed as constants in the RTL code under the TCMC-MUL architecture, the TCMC block, which realizes the multiplication of the input variable by a target or decoy constant at a time, is generated by the method of [18] under the TCMC-SA architecture.

#### IV. EXPERIMENTAL RESULTS

As an experiment set, three FIR filters, selected from the FIR filter benchmark suite [33], were used. Their specifications are given in Table I, where  $n$  and  $m$  are the number of filter coefficients and primary select inputs, respectively, and  $mbw$  is the maximum bit-width of filter coefficients. Note that  $\#in$  and  $\#out$  stand respectively for the number of inputs and outputs of the TCMC design computed when the bit-width of the filter input  $ibw$  is 32.

Conventional logic locking was applied to the combinational TCMC blocks of FIR filters under the *mux-mul* and

TABLE I  
SPECIFICATIONS OF FIR FILTERS AND TCMC BLOCKS.

Index	Filter Name	Coefficient Details			TCMC Details	
		n	m	mbw	#in	#out
1	Johansson08_30	30	5	10	37	42
2	Shi11_S2	60	6	10	38	42
3	Maskell07_A108	108	7	9	39	41

*mux-add* architectures, while the proposed technique was used to obfuscate these combinational TCMC blocks under the TCMC-MUL and TCMC-SA architectures. Logic synthesis was performed by Cadence Genus using a commercial 65nm cell library. The functionality of designs was verified on 10,000 randomly generated input signals in simulation, from which the switching activity information is collected and utilized by the synthesis tool to compute power dissipation. The SAT and automatic test pattern generation (ATPG) based attacks developed in [25] were used to check the resiliency of locked and obfuscated TCMC designs after they were synthesized into a gate-level netlist. Note that the ATPG based attack of [25] initially uses ATPG methods to determine key inputs and then, the SAT based attack to find the rest of key inputs undetermined by ATPG methods. As a common practice, a time limit of 1 day was given to the attacks which were run on a computing cluster including Intel Xeon processing units at 2.4GHz with 40 cores and 96GB memory.

Tables II and III present the gate-level design results of locked and obfuscated combinational TCMC blocks, respectively, when  $ibw$  is 32. The number of key inputs  $p$  is 32, 64, and 128 for the FIR filter *Johansson08\_30*, *Shi11\_S2*, and *Maskell07\_A108*, respectively. In these tables, *area*, *delay*, and *power* stand for the total area in  $\mu m^2$ , delay in the critical path in  $ps$ , and total power dissipation in  $\mu W$ , respectively. Also, ASAT and AATPG denote the SAT and ATPG based attacks, respectively, where *time* is their run-time in seconds. In Table II, *LLT* denotes a logic locking technique, where RAND, IOLTS, SAR, and SFL1<sup>1</sup> are the methods of [9], [10], [26], and [8], respectively.

Observe from Table II that while the TCMC designs locked by RAND, IOLTS and SFL1 techniques are vulnerable to the SAT and ATPG based attacks, the SFL1 technique leads to locked designs which have larger hardware complexity than those of any other techniques used in this paper. Besides, the SAR method generates locked designs comparable to those generated by the IOLTS and RAND methods in terms of hardware complexity, but more resilient to the attacks. On the other hand, observe from Table III that the proposed obfuscation technique generates locked designs that the SAT and ATPG based attacks find hard to decrypt. Moreover, the designs obfuscated by the proposed technique have less hardware complexity than those locked by the SFL1 technique. When compared to the designs locked by the SAR technique<sup>2</sup>

<sup>1</sup>The  $h$  parameter of the SFL1-HD technique, which is used to adjust the tradeoff between SAT attack resiliency and output corruption, was set to  $p/4$  in our experiments.

<sup>2</sup>Designs locked by both SAR and the proposed obfuscation methods could not be decrypted by the SAT and ATPG based logic locking attacks in a given time-limit.

TABLE II  
RESULTS OF TCMC BLOCKS OF FIR FILTERS LOCKED BY PROMINENT TECHNIQUES.

Filter Index	Architecture	LLT	Synthesis Results			ASAT time	AATPG time
			area	delay	power		
1	mux-mul	RAND	2775	5558	1147	49743	22
		IOLTS	2802	4355	1229	>1day	>1day
		SAR	2927	4436	1225	>1day	>1day
		SFLL	4020	4473	2391	301	100
	mux-add	RAND	3071	6336	1393	65002	1377
		IOLTS	2894	5234	1386	>1day	>1day
2	mux-mul	RAND	3104	5588	1334	>1day	18
		IOLTS	3035	4558	1279	>1day	>1day
		SAR	3168	4603	1236	>1day	>1day
		SFLL	5648	6290	4998	>1day	>1day
	mux-add	RAND	3570	6661	1536	>1day	>1day
		IOLTS	3260	5939	1400	>1day	>1day
3	mux-mul	RAND	3020	6268	1186	50758	33327
		IOLTS	2759	4765	1112	21104	23423
		SAR	3070	4945	1121	>1day	>1day
		SFLL	9313	11629	17585	>1day	>1day
	mux-add	RAND	3913	6705	1126	10555	7254
		IOLTS	3462	5189	1099	19235	20885
		SAR	3703	5149	1070	>1day	>1day
		SFLL	10000	11909	17487	>1day	>1day

TABLE III  
RESULTS OF TCMC BLOCKS OF FIR FILTERS OBFUSCATED BY THE PROPOSED TECHNIQUE.

Filter Index	Architecture	Synthesis Results			ASAT time	AATPG time
		area	delay	power		
1	TMCM-MUL	2749	5341	1170	>1day	>1day
	TMCM-SA	3445	6651	2024	>1day	>1day
2	TMCM-MUL	4362	5810	3546	>1day	>1day
	TMCM-SA	4318	7139	2169	>1day	>1day
3	TMCM-MUL	4595	5636	3522	>1day	>1day
	TMCM-SA	4155	6256	1895	>1day	>1day

under the *mux-mul* architecture, the area, delay, and power dissipation can increase up to 49%, 26%, and 214% in the obfuscated TCMC designs under the TMCM-MUL architecture. However, the obfuscation technique can find a TCMC design with less area on the filter *Johansson08\_30*. With respect to the synthesis results of designs locked by the SAR technique under the *mux-add* architecture, the area, delay, and power dissipation can increase up to 27%, 29%, and 77% in the obfuscated designs under the TMCM-SA architecture. However, we note that the main advantage of the proposed obfuscation method is to protect the target constants from reverse engineering, which cannot be guaranteed by a traditional logic locking technique. Also, SAR has an extremely low impact on circuit functionality, meaning that for each input pattern, there is only one key value that leads to corruption at outputs, whereas, our method has a high impact as shown in Fig. 7. Furthermore, observe from Table III that the TMCM-SA architecture can lead to designs with less area and power consumption when compared to the TMCM-MUL architecture, e.g., the FIR filter *Shi11\_S2* and *Maskell07\_A108*. The delay of obfuscated designs under the TMCM-SA architecture is generally larger than that of designs under the TMCM-MUL architecture because of a large number of operations in series in the TCMC blocks obtained by the algorithm of [18].

To explore the impact of the number of key inputs on the hardware complexity and resiliency to the attacks of

TABLE IV  
IMPACT OF THE NUMBER OF KEY INPUTS IN THE PROPOSED OBFUSCATION TECHNIQUE.

$p$	Architecture	Synthesis Results			ASAT time	AATPG time
		area	delay	power		
16	TMCM-MUL	2688	5390	1084	773	26
	TMCM-SA	3398	5442	1647	>1day	34
32	TMCM-MUL	2749	5341	1170	>1day	>1day
	TMCM-SA	3445	6651	2024	>1day	>1day
48	TMCM-MUL	2862	5696	1282	>1day	>1day
	TMCM-SA	3611	6586	1720	>1day	>1day
64	TMCM-MUL	4420	5762	3132	>1day	>1day
	TMCM-SA	3697	7224	1874	>1day	>1day
80	TMCM-MUL	4631	5656	3241	>1day	>1day
	TMCM-SA	4515	7618	2990	>1day	>1day

TABLE V  
IMPACT OF THE BIT-WIDTH OF FILTER INPUT IN THE PROPOSED OBFUSCATION TECHNIQUE.

$ibw$	Architecture	Synthesis Results			ASAT time	AATPG time
		area	delay	power		
16	TMCM-MUL	2145	3611	980	177	17902
	TMCM-SA	2741	5291	1269	409	1181
20	TMCM-MUL	2589	4670	1466	1369	>1day
	TMCM-SA	3127	5691	1555	2682	3626
24	TMCM-MUL	3144	4603	1970	28003	>1day
	TMCM-SA	3507	6159	1802	13148	7848
28	TMCM-MUL	3836	5000	2700	>1day	>1day
	TMCM-SA	3855	6644	2087	27221	31877
32	TMCM-MUL	4362	5810	3546	>1day	>1day
	TMCM-SA	4318	7139	2169	>1day	>1day

the obfuscated designs, the TCMC block of the FIR filter *Johansson08\_30* is implemented with a  $p$  value in between 16 and 80, increased in a step of 16. Table IV shows the synthesis results of TCMC designs and solutions of the attacks.

Observe from Table IV that as  $p$  increases, the hardware complexity of the obfuscated designs is increased. However, the increase ratio in area and power dissipation of the designs under the TMCM-MUL architecture is larger than that of the designs under the TMCM-SA architecture, such that the area and power dissipation of the design under the TMCM-SA architecture become smaller than those of designs under the TMCM-MUL architecture as  $p$  increases. This is because as  $p$  increases, the size of multiplexors increases under the TMCM-MUL architecture and the complexity of the TCMC design under the TMCM-SA architecture increases slightly due to the optimization algorithm of [18]. Also, as  $p$  decreases, the obfuscated TCMC design becomes less resilient to attacks.

To find the impact of the filter input bit-width on the hardware complexity and resiliency to the attacks of the obfuscated designs, the TCMC block of the FIR filter *Shi11\_S2* is designed when  $p$  is 64 and  $ibw$  is in between 16 and 32, increased in a step of 4. Table V shows the synthesis results of the obfuscated TCMC designs and solutions of the attacks.

Observe from Table V that as  $ibw$  increases, the hardware complexity of the TCMC designs increases since the size of operators increases. Note that the size of a multiplier under the TMCM-MUL architecture has a larger impact on the hardware complexity when compared to the size of adders, subtractors, and adders/subtractors under the TMCM-SA architecture since area and power dissipation of designs under the TMCM-MUL architecture become larger than those of designs under the TMCM-SA architecture as  $ibw$  increases. Observe that the resiliency of obfuscated designs to the attacks also increases



TABLE VI  
IMPACT OF THE DECOY SELECTION METHOD IN THE PROPOSED  
OBFUSCATION TECHNIQUE.

Filter Index	Architecture	DSM	Synthesis Results			ASAT	AATPG
			area	delay	power	time	time
1	TMCN-MUL	random	4382	5388	3115	>1day	3580
		proposed	2749	5341	1170	>1day	>1day
	TMCN-SA	random	3489	5360	1767	>1day	>1day
		proposed	3445	6651	2024	>1day	>1day
2	TMCN-MUL	random	4740	5756	3784	>1day	>1day
		proposed	4362	5810	3546	>1day	>1day
	TMCN-SA	random	4475	6208	1800	26299	42029
		proposed	4318	7139	2169	>1day	>1day
3	TMCN-MUL	random	4833	5756	3442	>1day	>1day
		proposed	4595	5636	3522	>1day	>1day
	TMCN-SA	random	4073	7529	1644	42414	>1day
		proposed	4155	6256	1895	>1day	>1day

TABLE VII

IMPACT OF OBFUSCATION IN THE FOLDED FIR FILTER DESIGN.

Filter Index	Technique	Architecture	Synthesis Results		
			area	delay	power
1	Original	<i>mux-mul</i>	14082	6362	1386
		<i>mux-add</i>	14396	6797	1592
	Obfuscated	TMCN-MUL	14171	6101	1386
		TMCN-SA	14973	7548	1969
2	Original	<i>mux-mul</i>	25007	6045	2011
		<i>mux-add</i>	25485	6789	2242
	Obfuscated	TMCN-MUL	26486	6298	2382
		TMCN-SA	26813	8172	2722
3	Original	<i>mux-mul</i>	41391	6260	3200
		<i>mux-add</i>	42238	6652	3228
	Obfuscated	TMCN-MUL	43379	6568	3630
		TMCN-SA	43738	8422	4083

as *ibw* increases. This is mainly because the search space of the problem of finding key inputs increases as *ibw* increases.

To explore the impact of the decoy selection method (DSM) on the hardware complexity and resiliency to the attacks of the obfuscated designs, the TMCN blocks of FIR filters are also implemented when decoys are chosen randomly, respecting *mbw*. In these designs, *ibw* is 32 and *p* is 32, 64, and 128 for the FIR filter *Johansson08\_30*, *Shi11\_S2*, and *Maskell07\_A108*, respectively. Table VI presents the synthesis results of the obfuscated TMCN designs obtained using different DSMs and the solutions of the attacks.

Observe from Table VI that because the proposed DSM favors unique decoy constants with a small Hamming distance value with respect to the associated target constant, it generally leads to obfuscated TMCN designs with a smaller area when compared to the random decoy selection under both design architectures, except the FIR filter *Maskell07\_A108* under the TMCN-SA architecture. Random decoy selection can also create vulnerabilities on the key inputs which is anticipated due to the use of common decoys for different target constants.

To investigate the impact of obfuscation of the TMCN block in filter design, these FIR filters are implemented as shown in Fig. 5(b) when their TMCN blocks are realized under the *mux-mul* and *mux-add* architectures and these designs are compared with filters including the obfuscated TMCN blocks generated under the TMCN-MUL and TMCN-SA architectures. Table VII shows the synthesis results obtained when *ibw* is 32 and *p* is 32, 64, and 128 for the FIR filter *Johansson08\_30*, *Shi11\_S2*, and *Maskell07\_A108*, respectively.

Observe from Table VII that the hardware obfuscation on the TMCN block of an FIR filter under the TMCN-MUL

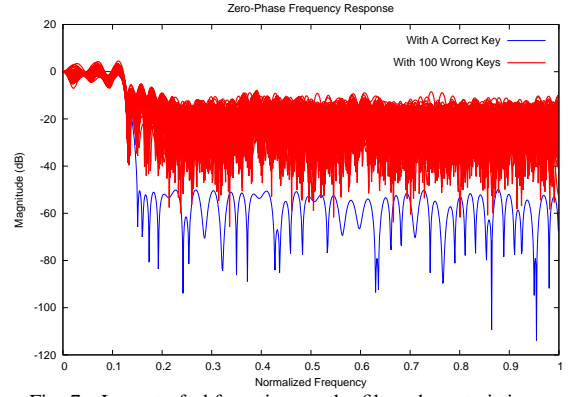


Fig. 7. Impact of obfuscation on the filter characteristics.

(TMCN-SA) architecture can respectively increase the area, delay, and power dissipation up to 5.5% (4.9%), 4.6% (21.0%), and 15.5% (20.9%) when compared to the original FIR filters under the *mux-mul* (*mux-add*) architecture. Note that the TMCN block has less impact on the area of a folded FIR filter with respect to the registers. Hence, an FIR filter can be obfuscated with a small increase in area.

As opposed to existing logic locking techniques, measuring bit-level corruption at the outputs is not an appropriate metric for a filter. Instead, to explore the impact of decoys on the filter behavior, its zero-phase frequency response is computed based on the original coefficients and the constants selected randomly from the original coefficients and decoys. Fig. 7 shows the behavior of the filter *Maskell07\_A108* when *p* is 128 and a correct (blue) and 100 wrong (red) keys are applied.

Observe from Fig. 7 that the decoys can alter the filter design characteristics, obfuscating the filter behavior. Note that decoys can be selected to change the filter behavior completely under each possible wrong key, considering also the hardware complexity and resiliency to the logic locking attacks.

## V. CONCLUSIONS

This paper presented a hardware obfuscation technique that prevents an adversary at an untrusted foundry from reverse engineering the constants of a TMCN block, a fundamental operation in the folded design of many IPs, such as ANNs and DSP circuits. The proposed technique obfuscates the target constants of the TMCN block using unique decoy constants and additional logic with keyed inputs. The obfuscation process takes place at RTL before logic synthesis, rather than at gate-level as in traditional logic locking schemes. It is observed that the proposed technique generates obfuscated TMCN designs that are resilient to well-known logic locking attacks. The proposed design architectures introduce alternative realizations of the TMCN block with different hardware complexity and resiliency to the attacks, enabling a designer to choose the one that fits best in an application. In any case, **the true IP** of these designs, i.e., the constants themselves, can be protected.

As a future work, the impact of synthesis optimizations on the hardware complexity and resiliency of the obfuscated designs is being explored.

## ACKNOWLEDGMENT

This work has been partially conducted in the project “ICT programme” which was supported by the European Union through the European Social Fund. It was also partially supported by European Union’s Horizon 2020 research and innovation programme under grant agreement No 952252 (SAFEST) and by the Estonian Research Council grant MOBERC35.

## REFERENCES

- [1] Defence Science Board Task Force. (2015, February) On High Performance Microchip Supply Chain. [Online]. Available: <https://dsb.cto.mil/reports/2000s/ADA435563.pdf>
- [2] R. Torrance and D. James, “The State-of-the-Art in Semiconductor Reverse Engineering,” in *DAC*, 2011, p. 333–338.
- [3] R. Karri, J. Rajendran, K. Rosenfeld, and M. Tehranipoor, “Trustworthy Hardware: Identifying and Classifying Hardware Trojans,” *Computer*, vol. 43, no. 10, p. 39–46, 2010.
- [4] A. B. Kahng, J. Lach, W. H. Mangione-Smith, S. Mantik, I. L. Markov, M. Potkonjak, P. Tucker, H. Wang, and G. Wolfe, “Watermarking Techniques for Intellectual Property Protection,” in *DAC*, 1998, pp. 776–781.
- [5] F. Koushanfar and G. Qu, “Hardware Metering,” in *DAC*, 2001, pp. 490–493.
- [6] J. Rajendran, M. Sam, O. Sinanoglu, and R. Karri, “Security Analysis of Integrated Circuit Camouflaging,” in *ACM SIGSAC Conference on Computer and Communications Security*, 2013, p. 709–720.
- [7] J. Rajendran, Y. Pino, O. Sinanoglu, and R. Karri, “Security Analysis of Logic Obfuscation,” in *DAC*, 2012, pp. 83–89.
- [8] M. Yasin, A. Sengupta, M. T. Nabeel, M. Ashraf, J. Rajendran, and O. Sinanoglu, “Provably-Secure Logic Locking: From Theory To Practice,” in *ACM SIGSAC Conference on Computer and Communications Security*, 2017, p. 1601–1618.
- [9] J. A. Roy, F. Koushanfar, and I. L. Markov, “EPIC: Ending Piracy of Integrated Circuits,” in *DATE*, 2008, pp. 1069–1074.
- [10] S. Dupuis, P. Ba, G. Di Natale, M. Flottes, and B. Rouzeyre, “A Novel Hardware Logic Encryption Technique for Thwarting Illegal Overproduction and Hardware Trojans,” in *IOLTS*, 2014, pp. 49–54.
- [11] A. Baumgarten, A. Tyagi, and J. Zambreno, “Preventing IC Piracy Using Reconfigurable Logic Barriers,” *IEEE Design Test of Computers*, vol. 27, no. 1, pp. 66–75, 2010.
- [12] R. Ding, Z. Liu, R. D. S. Blanton, and D. Marculescu, “Quantized Deep Neural Networks for Energy Efficient Hardware-based Inference,” in *ASP-DAC*, 2018, pp. 1–8.
- [13] Y. J. Yu and Y. C. Lim, “Optimization of Linear Phase FIR Filters in Dynamically Expanding Subexpression Space,” *Circuits, Systems, and Signal Processing*, vol. 29, no. 1, pp. 65–80, 2010.
- [14] N. Nedjah, R. M. da Silva, L. M. Mourelle, and M. V. C. da Silva, “Dynamic MAC-based Architecture of Artificial Neural Networks Suitable for Hardware Implementation on FPGAs,” *Neurocomputing*, vol. 72, no. 10, pp. 2171 – 2179, 2009.
- [15] S. Mirzaei, A. Hosangadi, and R. Kastner, “FPGA Implementation of High Speed FIR Filters Using Add and Shift Method,” in *International Conference on Computer Design*, 2006, pp. 308–313.
- [16] K. Parhi, *VLSI Digital Signal Processing Systems: Design and Implementation*. John Wiley & Sons, 1999.
- [17] P. Tummelshammer, J. Hoe, and M. Püschel, “Time-Multiplexed Multiple-Constant Multiplication,” *IEEE TCAD*, vol. 26, no. 9, pp. 1551–1563, 2007.
- [18] L. Aksoy, P. Flores, and J. Monteiro, “Multiplierless Design of Folded DSP Blocks,” *ACM Transactions on Design Automation of Electronic Systems*, vol. 20, no. 1, 2014.
- [19] H. Nguyen and A. Chatterjee, “Number-Splitting with Shift-and-Add Decomposition for Power and Hardware Optimization in Linear DSP Synthesis,” *IEEE TVLSI*, vol. 8, no. 4, pp. 419–424, 2000.
- [20] M. Ercegovic and T. Lang, *Digital Arithmetic*. Morgan Kaufmann, 2003.
- [21] L. Aksoy, P. Flores, and J. Monteiro, “A Tutorial on Multiplierless Design of FIR Filters: Algorithms and Architectures,” *Circuits, Systems, and Signal Processing*, vol. 33, no. 6, p. 1689–1719, 2014.
- [22] L. Aksoy, E. O. Güneş, and P. Flores, “Search Algorithms for the Multiple Constant Multiplications Problem: Exact and Approximate,” *Elsevier Microprocessors and Microsystems*, vol. 34, no. 5, p. 151–162, 2010.
- [23] L. Wanhammar, *DSP Integrated Circuits*. Academic Press, 1999.
- [24] K. Z. Azar, H. M. Kamali, H. Homayoun, and A. Sasan, “Threats on Logic Locking: A Decade Later,” 2019. [Online]. Available: <http://arxiv.org/abs/1905.05896>
- [25] P. Subramanyan, S. Ray, and S. Malik, “Evaluating the Security of Logic Encryption Algorithms,” in *HOST*, 2015, pp. 137–143.
- [26] M. Yasin, B. Mazumdar, J. J. V. Rajendran, and O. Sinanoglu, “SAR-Lock: SAT Attack Resistant Logic Locking,” in *HOST*, 2016, pp. 236–241.
- [27] R. S. Chakraborty and S. Bhunia, “HARPOON: An Obfuscation-Based SoC Design Methodology for Hardware Protection,” *IEEE TCAD*, vol. 28, no. 10, p. 1493–1502, 2009.
- [28] C. Pilato, F. Regazzoni, R. Karri, and S. Garg, “TAO: Techniques for Algorithm-Level Obfuscation during High-Level Synthesis,” in *DAC*, 2018.
- [29] S. A. Islam, L. K. Sah, and S. Katkooi, “High-Level Synthesis of Key-Obfuscated RTL IP with Design Lockout and Camouflaging,” *ACM TODAES*, vol. 26, no. 1, 2020.
- [30] Y. Lao and K. K. Parhi, “Obfuscating DSP Circuits via High-Level Transformations,” *IEEE TVLSI*, vol. 23, no. 5, pp. 819–830, 2015.
- [31] J. Sweeney, M. Zackriya, S. Pagliarini, and L. Pileggi, “Latch-Based Logic Locking,” in *HOST*, 2020, pp. 132–141.
- [32] G. Bottegal, F. Farokhi, and I. Shames, “Preserving Privacy of Finite Impulse Response Systems,” *IEEE Control Systems Letters*, vol. 1, no. 1, pp. 128–133, 2017.
- [33] FIRSuite. (2009) Suite of Constant Coefficient FIR Filters. [Online]. Available: <https://www.firsuite.net/>